RSC Advances

This article can be cited before page numbers have been issued, to do this please use: H. Sharma, N. Singh and D. O. Jang, *RSC Adv.*, 2014, DOI: 10.1039/C4RA12892C.

ROYAL SOCIETY OF CHEMISTRY

www.rsc.org/advances

View Article Online
DOI: 10.1039/C4RA12892C

Graphical Abstract

A benzimidazole/benzothiazole-based electrochemical chemosensor for nanomolar detection of guanine

Hemant Sharma, Narinder Singh,* and Doo Ok Jang*

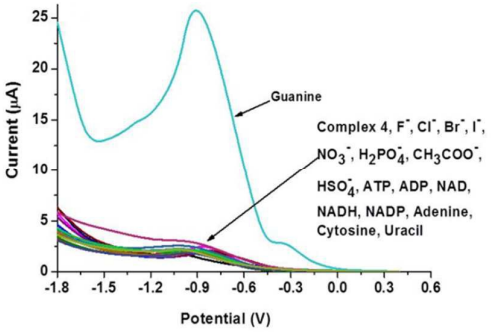

The electrochemical detection of guanine was accomplished using benzimidazole/ benzothiazole-based imine-linked Co(III) complexes with platinum electrodes.

A benzimidazole/benzothiazole-based electrochemical chemosensor for nanomolar detection of guanine

Hemant Sharma,[a] Narinder Singh[a,*] and Doo Ok Jang[b,*]

[a]Department of Chemistry, Indian Institute of Technology Ropar (IIT Ropar), Rupnagar, Panjab, India 140001

[b]Department of Chemistry, Yonsei University, Wonju 220-710, Republic of Korea

nsingh@iitrpr.ac.in; dojang@yonsei.ac.kr

Abstract: The electrochemical detection of guanine was accomplished using benzimidazole/ benzothiazole-based imine-linked Co(III) complexes **2**, **4** and **6** with platinum electrodes. Linear sweep voltammetry (LSV), differential pulse voltammetry (DPV) and cyclic voltammetry (CV) were the major analytical techniques used to explore the recognition behavior of the complexes. The detection limit, linear range of detection and sensitivity for complex **2** (16.6 nM, 3.5-10 μM and 4.01 μA μM^{-1} cm^2), complex **4** (13.4 nM, 5.0-120 μM and 3.18 μA μM^{-1} cm^2) and complex **6** (11.3 nM, 2.5-100 μM and 2.0 μA μM^{-1} cm^2) were calculated. Advantages of this methodology include simplicity, an unmodified electrode, high sensitivity and reproducibility.

Introduction

In recent years, biomolecular recognition has gained considerable attention due to its widespread role in biological, chemical and environmental systems.[1-8] The fundamentals of biomolecular recognition originate from the structure of deoxyribonucleic acid (DNA). DNA is a genetic material consisting of two strands, which are attached to each other through non-covalent interactions between nitrogenous bases (adenine, guanine, cytosine and thymine). These nitrogenous bases bind in a particular way, called complementary base paring.[9, 10] This complementary binding and non-covalent interaction are the basis for molecular recognition. Furthermore, nitrogenous bases are important compounds in biological systems because they are involved in several processes, including energy transduction, the storage of genetic information, metabolic cofactors and cell signaling.[11, 12]

The determination and estimation of nitrogenous bases are particular for guanine because it can be oxidized easily as compared to the other purine bases. Up to the present time, various analytical methods have been developed for the determination and estimation of nitrogenous bases as achieved by liquid chromatography, mass spectroscopy, UV-vis and fluorescence spectroscopy.[13-15] Electrochemical techniques offer several benefits over other detection techniques, including simplicity, relative low cost, portability, high performance with lower background, sensitivity and applicability to turbid samples. Various efforts regarding the electrochemical sensing of guanine have been reported, which used modified electrodes with different

View Article Online
DOI: 10.1039/C4RA12892C

electron transfer mediators such as cobalt hexacyanoferrate,[16] cobalt(II) phthalocyanine,[17] redox polymer[18] and cobalt oxide nanostructures[19]. However, these techniques have suffered from various limitations including a high detection limit, reduced stability of mediators and electro-catalysts, and lengthy, time-consuming preparation methods. We previously reported fluorogenic and chromogenic chemosensors for cations and anions using benzimidazole/benzothiazole-based signaling units.[20-22] Herein, we wish to report benzimidazole/benzothiazole-based Co(III) complexes for the direct sensing of guanine without modification of the surface of electrodes. To the best of our knowledge, this is the first attempt to use benzimidazole/benzothiazole-based sensors to recognize guanine via electrochemical techniques.

Experimental section

General

Chemicals were purchased from Aldrich and were used without further purification. The NMR spectra were recorded on JNM-ECS400 (JEOL) spectrophotometer operated at 400 MHz for ^{1}H NMR and 100 MHz for ^{13}C NMR spectra. The splitting patterns were visualized as s (singlet), bs (broad singlet), d (doublet), dd (doublet of doublet), t (triplet), and m (multiplet). The electrochemical measurements were recorded on a Potentiostat-Galvanostat BASI EPSILON. The X-ray diffraction (XRD) pattern was recorded with a PANalytical X'PERT PRO diffractometer, operated at 45 KV, 40 mA using Ni-filtered Cu- Kα radiations with a scan speed of 10º/min for 2θ in a range from 10 to 70.

Recognition studies

All recognition studies were performed at 25±1 ^{o}C, and before recording any spectrum, a sufficient incubation period with shaking was performed to ensure the uniformity of the solution. For binding studies, a stock solution of respective receptors was prepared in DMSO/H_2O or a THF/H_2O (8:2; v/v) solvent system. For binding studies, tetrabutylammonium anion salt (F^-, Cl^-, Br^-, I^-, NO_3^-, $H_2PO_4^-$, CH_3COO^- and HSO_4^-), sodium or disodium salt (ATP, ADP, NADH, NAD and NADP), and adenine, cytosine, guanine and uracil was employed. To perform this experiment, volumetric flasks (5 mL) were taken and each contained an analyte solution along with 10 μM of respective ligand solution and tetrabutylammonium perchlorate as the supporting electrolyte (0.1 M). Receptors showed selectivity and were titrated with the respective analyte. The titrations were performed in 10-mL volumetric flasks that contained a 10 μM solution of receptor and a different concentration of analyte. Furthermore, stoichiometry of the complex between the host and guest was revealed by a method of continuous variation or Job's plot, and was confirmed from mass spectroscopy. The interference studies were performed in 5 mL volumetric flasks, containing a solution of complex **2**, **4** or **6** along with guanine and an equal molar of particular competing an anion or a biomolecule. These solutions were kept for 1 h and then measurements were

View Article Online
DOI: 10.1039/C4RA12892C

carried out using desired techniques. Electrochemical detection was performed in a single-compartment cell under a nitrogen atmosphere at 25 ºC, with a Pt disk working electrode (3 mm diameter), a platinum wire counter electrode (0.5 mm diameter) and an $Ag/AgNO_3$ reference electrode. The Pt disk working electrode was abraded to a mirror finish using emery paper and α-Al_2O_3 (diameter of 50 nm). It was washed with distilled water followed by ultrasonic cleaning in ethanol and deionized water. Tetrabutylammonium perchlorate was used as the supporting electrolyte (0.1 M).

Synthesis of compound 1

A solution of 2-aminobenzimidazole (499 mg, 3.75 mmol) and 2,3-dihydroxybenzaldehyde (600 mg, 4.35 mmol) in methanol (20 mL) was heated to reflux for 10 h. A reddish-brown-colored compound was separated out when the reaction mixture was cooled to room temperature. After filtration, the solid was washed with methanol three times. This resulted in a 67% yield (640 mg); mp 244-245 °C; ^{1}H NMR (400 MHz, DMSO-d_6) δ 12.73 (bs, 1H, -OH), 11.93 (bs, 1H, -OH), 9.56 (s, 1H, -CH=N), 7.55-6.80 (m, 8H, Ar, NH); ^{13}C NMR (100 MHz, DMSO-d_6) δ 166.8, 154.3, 145.0, 146.3, 142.9, 134.5, 123.4, 122.9, 122.6, 120.7, 120.1, 119.9, 119.1, 111.8. Anal. Calcd. for $C_{14}H_{11}N_3O_2$: C, 66.40; H, 4.38; N, 16.59. Found: C, 66.34; H, 4.23; N, 16.71.

Synthesis of compound 2

A solution of compound **1** (678 mg, 2.68 mmol) and $Co(NO_3)_2$ (244 mg, 1.34 mmol) in THF (50 mL) was stirred at room temperature for 3 h. Tetrabutylammonium nitrate was added to the above solution for aerial oxidation. After filtration, a dark-brown-colored powder was obtained in 65% yield (980 mg). mp > 275 °C; ESI-MS (*m/z*): 618.3 $[M+1]^+$ for [**2**.$(H_2O)_3$]. Anal. Calcd. for $C_{28}H_{26}CoN_6O_7$: C, 54.46; H, 4.24; N, 13.61. Found: C, 54.61; H, 4.29, N, 13.59.

Synthesis of compound 3

A solution of 2-aminobenzothiazole (499 mg, 3.33 mmol) and salicylaldehyde (499 mg, 4.09 mmol) in methanol (20 mL) was heated to reflux for 10 h. A yellow-colored product was obtained when the reaction mixture was cooled to room temperature. After filtration, the product was obtained in 69% yield (583 mg). mp 135-136 °C; ^{1}H NMR (400 MHz, DMSO-d_6) δ 11.48 (s, 1H, -OH), 9.40 (s, 1H, -CH=N), 8.04 (d, J = 7.6 Hz, 1H, Ar), 7.91 (d, J = 8.0 Hz, 2H, Ar), 7.49 (t, J = 7.7 Hz, 2H, Ar), 7.42 – 7.37 (m, 1H, Ar), 7.02–6.94 (m, 2H, Ar); ^{13}C NMR (100 MHz, DMSO-d_6) δ 171.0, 166.3, 161.1, 151.7, 136.2, 134.5, 131.5, 127.3, 125.9, 123.1, 123.0, 120.4, 120.1, 117.5. Anal. Calcd. for $C_{14}H_{10}N_2OS$: C, 66.12; H, 3.96, N, 11.02. Found: C, 66.37, H, 3.85; N, 10.92.

View Article Online
DOI: 10.1039/C4RA12892C

Synthesis of compound 4

A solution of compound **3** (676 mg, 2.66 mmol) and $Co(NO_3)_2$ (244 mg, 1.34 mmol) in THF (50 mL) was stirred at room temperature for 3 h. Tetrabutylammonium nitrate was added to the above solution for aerial oxidation. After filtration, a dark-brown-colored product was obtained in 70% yield (1.05 g). mp 180-185 °C; ESI-MS (*m/z*): 565.0 $[M]^+$ for **4**. Anal. Calcd. for $C_{28}H_{18}CoN_4O_2S_2$: C, 59.47; H, 3.21; N, 9.91. Found: C, 59.44; H, 3.15; N, 9.89.

Synthesis of compound 5

A solution of 2-aminobenzothiazole (499 mg, 3.33 mmol) and 2-hydroxy-5-nitrobenzaldehyde (601 mg, 3.6 mmol) in methanol (20 mL) was heated to reflux for 10 h. A yellow-colored product was separated out when the reaction mixture was cooled to room temperature. After filtration, the product was obtained in 62% yield (617 mg). mp 220-221 °C; ^{1}H NMR (400 MHz, DMSO-d_6) δ 10.26 (s, 1H, -OH), 8.38 (d, J = 2.8 Hz, 1H, -CH=N), 8.31 (dd, J = 9.1, 2.9 Hz, 1H, Ar), 7.60 (d, J = 7.7 Hz, 1H, Ar), 7.45 (s, 1H, Ar), 7.28 (d, J = 7.9 Hz, 1H, Ar), 7.19 – 7.11 (m, 2H, Ar), 6.96 (t, J = 7.5 Hz, 1H, Ar); ^{13}C NMR (100 MHz, DMSO-d_6) δ 189.6, 167.0, 166.3, 165.0, 153.1, 140.2, 131.3, 126.0, 124.9, 122.7, 121.4, 121.4, 119.0, 118.2. Anal. Calcd. for $C_{14}H_9N_3O_3S$: C, 56.18; H, 3.03; N, 14.04. Found: C, 56.39; H, 3.05; N, 13.99.

Synthesis of compound 6

A solution of compound **5** (795 mg, 2.66 mmol) and $Co(NO_3)_2$ (244 mg, 1.34 mmol) in THF (50 mL) was stirred at room temperature for 3 h. Tetrabutylammonium nitrate was added to the above solution for aerial oxidation. After filtration, a dark-brown-colored powder was obtained in 60% yield (1.04 g). mp > 275 °C; ESI-MS (*m/z*): 724.5 $[M+1]^+$ for [**6**.$(H_2O)_2CH_3OH$]. Anal. Calcd. for $C_{29}H_{24}CoN_6O_9S_2$: C, 48.14; H, 3.34; N, 11.61. Found: C, 48.43; H, 3.66; N, 11.71.

Results and Discussion

Synthesis of receptors and cobalt complexes

Benzimidazole/benzothiazole-based imine-linked receptors **1**, **3** and **5** were prepared by condensation reactions. The condensation reactions of 2-aminobenzimidazole or 2-aminobenzothiazole with benzaldehyde derivatives were performed in methanol (Scheme 1). The products were obtained in good yields and characterized in agreement with the structures. To make them electrochemically active, cobalt complexes of receptors **1**, **3** and **5** were synthesized and characterized by mass spectroscopy and elemental analysis.

View Article Online
DOI: 10.1039/C4RA12892C

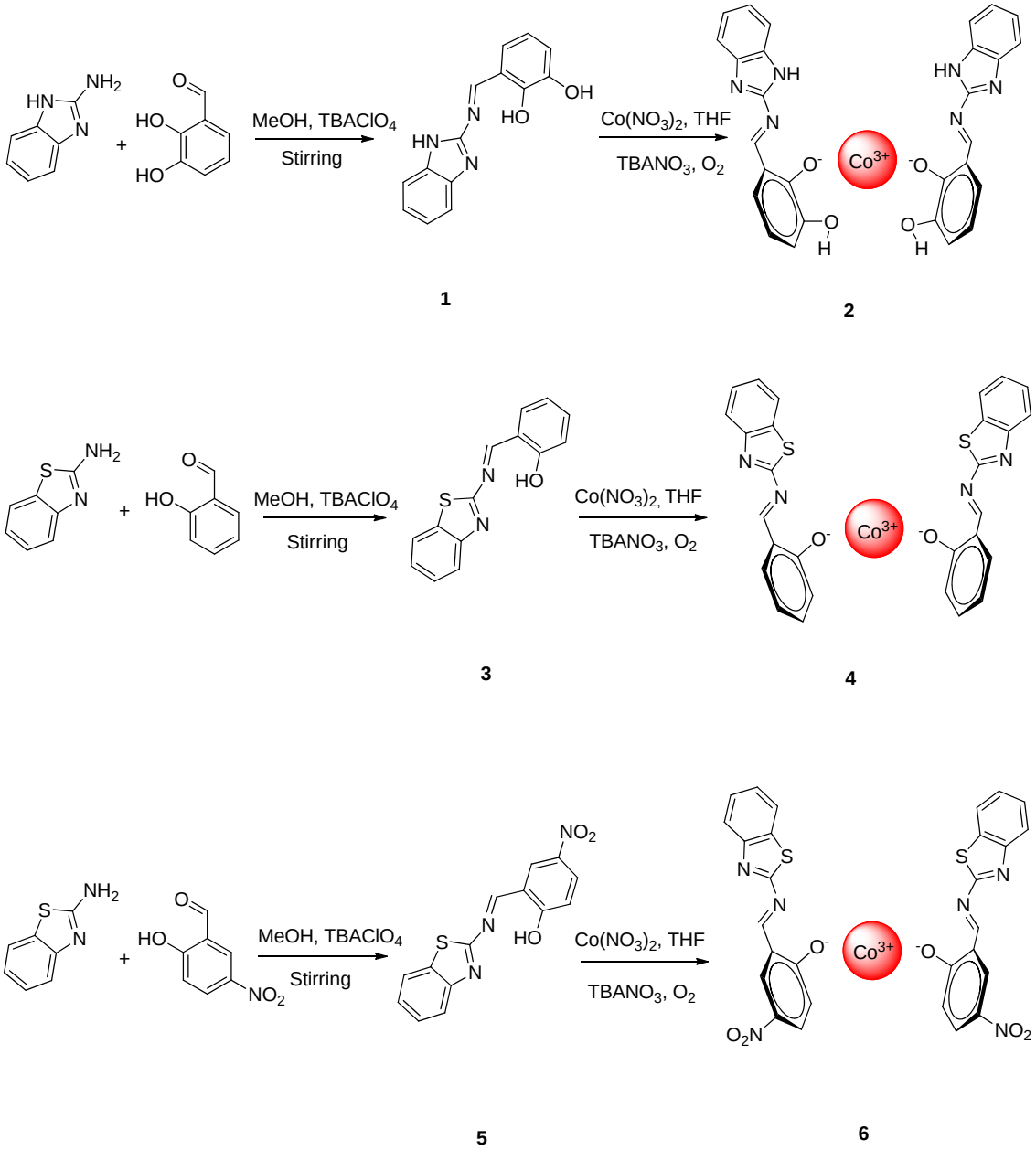

Scheme 1. Synthesis of receptors and cobalt complexes.

Among the various transition metals, cobalt was chosen because Co(III) was expected to act as a strong Lewis acid and show good electrochemical responses to the binding of analytes.[23] Powder X-ray diffraction (PXRD) was employed to analyze cobalt complexes **2**, **4** and **6**. Figure S1 illustrates that the diffraction patterns of Co(III) complexes **2**, **4** and **6** match neither receptors **1**, **3** and **5** nor cobalt nitrate. The stoichiometry of Co(III) complexes **2**, **4** and **6** were confirmed by mass spectroscopy (Figures S8-S10). The analysis of mass spectra of complexes **2**, **4** and **6** showed a 2:1 ratio between the receptor and Co(III).

Electrochemical detection of guanine

Benzimidazole/benzothiazole-based imine-linked Co(III) complexes **2**, **4** and **6** were expected to have high affinity towards anions and biomolecules by virtue of +3 oxidation state of cobalt and availability of H-bonding sites (N or NH) of the complexes, as shown in Scheme 1. Platinum electrode was employed as working electrode due to its robustness, versatility and behaviors as a noble metal. It provides more inert surface than others.[24] Linear sweep voltammetry (LSV) profile of complex **2** was recorded in the presence of various anions (F^-, Cl^-, Br^-, I^-, NO_3^-, $H_2PO_4^-$, CH_3COO^- and HSO_4^-) and biomolecules (ATP, ADP, NAD, NADH, NADP, adenine, guanine, cytosine and uracil) in a DMSO/H_2O (8:2, v/v) solvent system (Figure S11). Addition of guanine shifted the oxidation potential of complex **2**. But the responses were not selective; other anions/biomolecules also interfered. However, differential pulse voltammetry (DPV) profile of complex **2** showed a significant change upon addition of guanine (Figure 1A). It was observed that complex **2** has a peak at -0.752 V. Addition of analytes, with the exception of guanine, did not cause any shift in the potential of complex **2**. The addition of guanine produced a significant change in the oxidation potential of complex **2**. Two new peaks arose at -0.552 V and -1.132 V with high current intensity. Furthermore, differential pulse voltammograms of complex **2** and complex **2** + guanine were compared with guanine only (blank) as shown in Figure 1B. The voltammogram of guanine alone did not show any resemblance to the other complexes, which authenticated the binding between complex **2** and guanine.

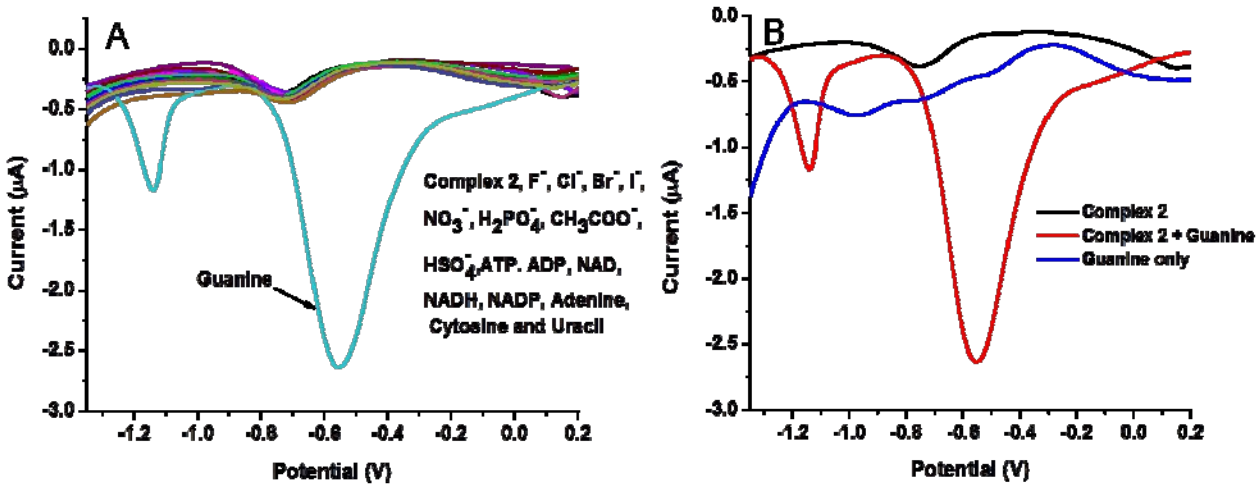

Figure 1. (A) Changes in the DPV profile of complex **2** (10 μM) in the presence of various tetrabutylammonium anion salts and biomolecules (30 μM) in a DMSO/H_2O (8:2, v/v) solvent system; (B) Comparison of DPV profile of complex **2**, complex **2** + guanine, and guanine only (blank) in a DMSO/H_2O (8:2, v/v) solvent system.

View Article Online
DOI: 10.1039/C4RA12892C

Cyclic voltammetry (CV) profiles of complex **2** were recorded in the presence and absence of guanine (Figure 2). Complex **2** has an E_{pc} and E_{pa} at -0.766 V and -0.890 V; however, the addition of guanine led to significant change in the anodic peak and a simultaneous shift in the cathodic potential, as shown in Figure 2. The cyclic voltammograms of complex **2** at different scan rates (25, 50, 75, 100 and 120) were recorded. The calibration plot was plotted between peak current and square root of scan rate and linear relationship was observed (Figure 2B). The linear relationship indicates that the process is controlled by a diffusion process.

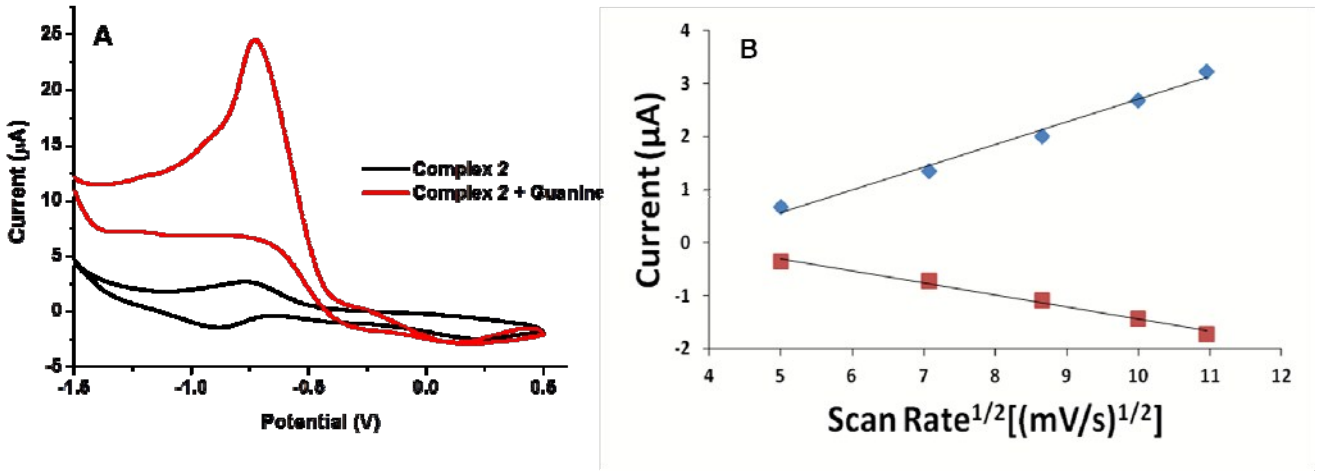

Figure 2. (A) Cyclic voltammogram of complex **2** (10 μM) with or without guanine (30 μM) in a DMSO/H_2O (8:2, v/v) solvent system; (B) Calibration plot of complex **2** showing peak current versus square root of scan rate (25, 50, 75, 100 and 120). Blue points represent current at -0.776 V and red points represent the current at -0.888 V.

To check the authenticity of binding, a titration was performed with complex **2** and guanine using a DPV (Figure 3). The titration results revealed that the oxidation potential of complex **2** was shifted towards higher potential, yielding a new peak at -0.552 V. Another peak was observed at -1.132 V. The plot was drawn between peak current and concentration of guanine (C_g) which showed a linear relationship in the concentration range of 3.5-10 μM as shown in the inset of Figure 3.

The detection limit was calculated using the signal to noise ratio (3σ) method, and it was about 16.6 nM. The linear regression equation was $I_{pa}(\mu A) = -0.284C_g(\mu M) + 0.802$, $R^2 = 0.993$. In addition, the recognition of guanine in the presence of competing molecules was performed by measuring the current at -0.552 V (Figure 4). For the selectivity study, a set of solutions were prepared that had an equal equivalent of guanine and other competing molecules along with 10 μM complex **2**. After incubation for 1 h, the DPV profile of these solutions was recorded. A graph of the peak current at -0.552 V against various solutions was plotted. The graph showed that complex **2** adequately recognized guanine even in the presence of other competing molecules, indicating the high selectivity of complex **2**.

View Article Online
DOI: 10.1039/C4RA12892C

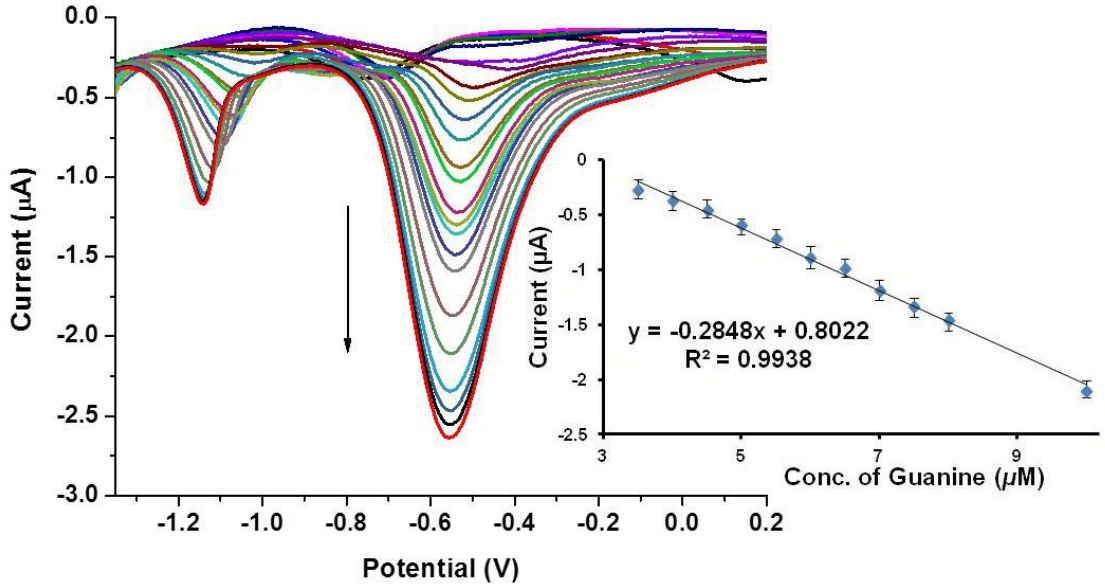

Figure 3. DPV curves of complex **2** (10 μM) in different concentrations of guanine (0 to 30 μM) in DMSO/H_2O (8:2, v/v). The inset represents the linear relationship between the peak current at -0.552 V versus the concentration of guanine.

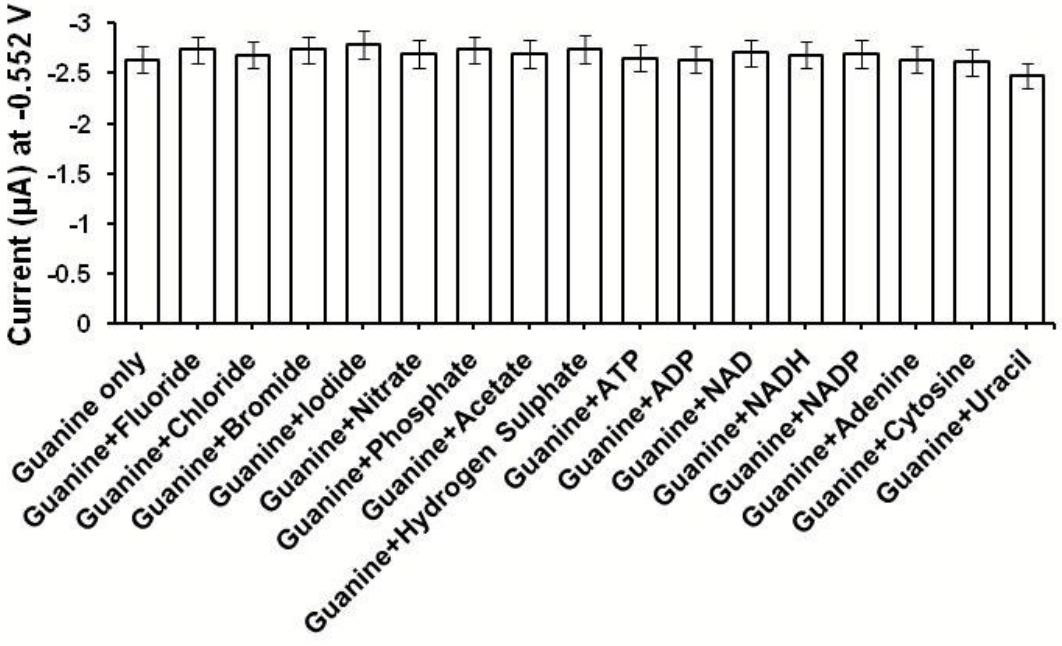

Figure 4. Influence on the peak current of complex **2** (10 μM) in the presence of guanine along with equal molar amounts of various competing anions and biomolecules in a DMSO/H_2O (8:2, v/v) solvent system.

View Article Online
DOI: 10.1039/C4RA12892C

Binding interactions of benzothiazole-derived complexes **4** and **6** with a variety of anions and biomolecules were accomplished using linear sweep voltammetry (LSV) and CV. All recognition studies of complex **4** were recorded in a DMSO/H_2O (8:2, v/v) solvent system. Figure 5A exemplified the binding behavior of complex **4** towards anions and biomolecules using LSV. Only guanine caused a change in the oxidation potential of complex **4**. From the titration experiments, it was observed that the addition of 5 μM of guanine led to an enhancement at -0.435 V. Upon continuing the titration, the anodic peak at -0.435 V was shifted toward lower potential and finally stabilized at -0.941 V. The addition of guanine was found to enhance the current intensity only at -0.941 V (Figure 5B). A plot was drawn between the anodic peak current at -0.941 V versus concentration of guanine, and resulted in a linear relationship in the concentration range of 5 to 120 μM, as shown in inset of Figure 5B. The linear regression equation is $I_{pa}(\mu A) = 0.225C_g(\mu M) - 0.5994$, $R^2 = 0.984$. The detection limit was approximately 13.4 nM, as calculated by the signal to noise ratio (3σ) method.

Figure 5. (A) Linear sweep voltammogram of complex **4** (10 μM) in the presence of various tetrabutylammonium anion salts and biomolecules (150 μM) in a DMSO/H_2O (8:2, v/v) solvent system; (B) Successive changes in the LSV profile of complex **4** upon titration with guanine (0 to 150 μM); the inset represents the linear relationship between the current intensity at -0.941 V and the concentration of guanine.

The CV also illustrated the high sensitivity of complex **4** towards guanine. A small amount of guanine (5 μM) triggered a huge change in the redox potential of complex **4** (Figure 6A). The cyclic voltammogram of the blank solution (guanine only) was recorded and compared with complex **4** and complex **4** + guanine, confirming the high affinity of complex **4** for guanine. The linear relationship was observed between peak current and square root of scan rate, indicating a diffusion process (Figure 6B). To examine the interference of

View Article Online
DOI: 10.1039/C4RA12892C

other analytes, recognition of guanine in the presence of an equal equivalent of other competing molecules was performed (Figure 7). Complex **4** recognized the guanine even in the presence of other competing molecules.

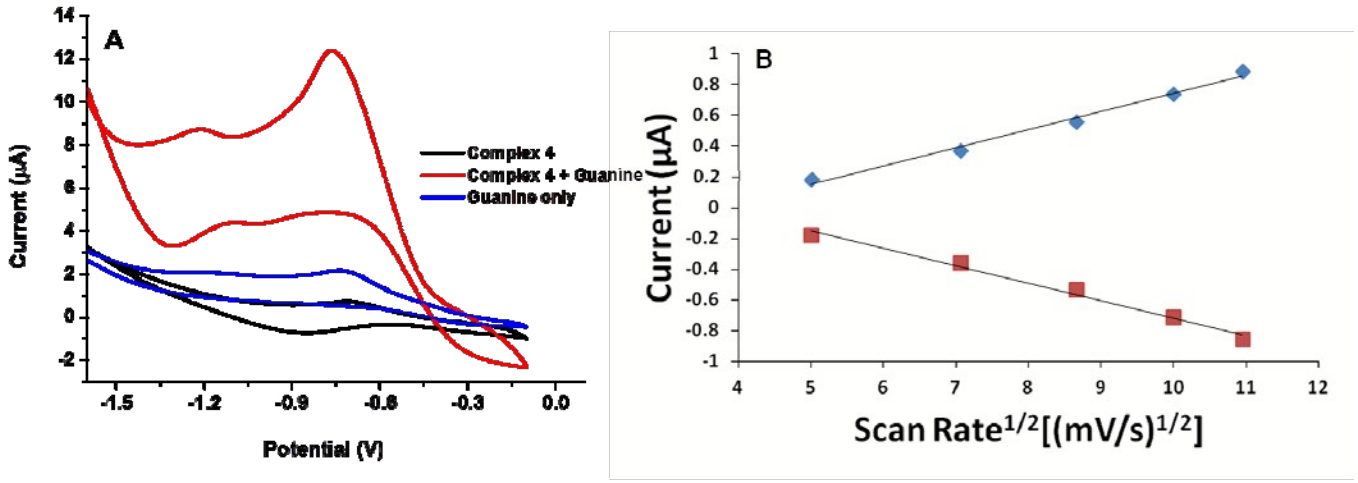

Figure 6. (A) CV profile of complex **4** (10 μM), complex **4** + guanine (5 μM), and guanine only (50 μM) (blank) in a DMSO/H_2O (8:2, v/v) solvent system; (B) Calibration plot of complex **4** showing peak current versus square root of scan rate (25, 50, 75, 100 and 120). Blue points represent current at -0.715 V and red points represent the current at -0.851 V.

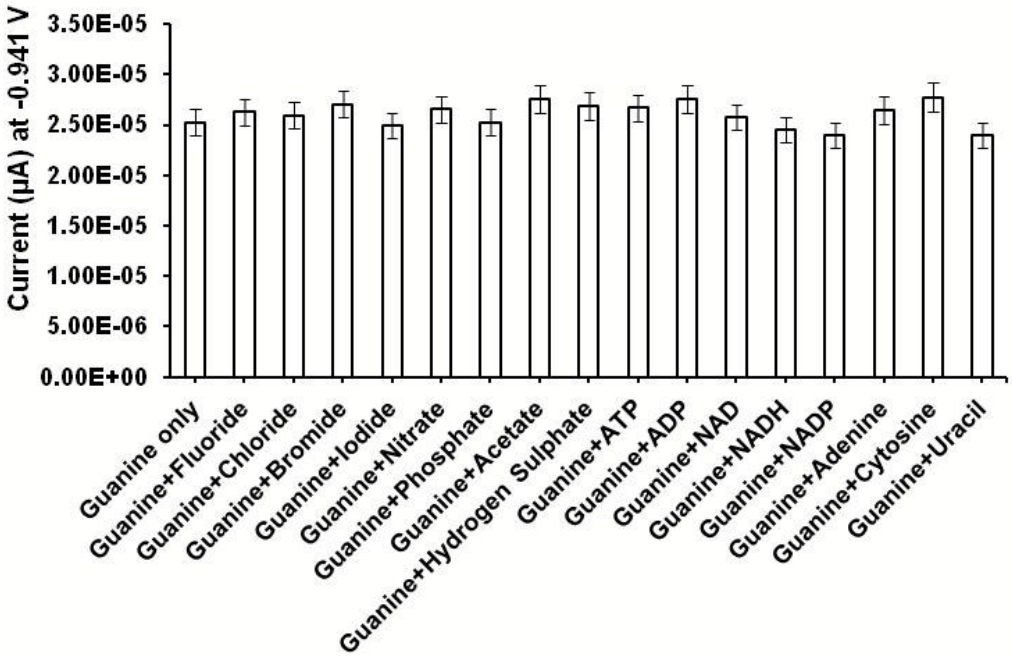

Figure 7. Effect on the peak current of complex **4** at -0.941 V in the presence of guanine along with equal molar amounts of various competing anions and biomolecules in DMSO/H_2O (8:2, v/v).

Recognition studies of complex **6** were executed in a THF/H_2O (8:2, v/v) solvent system. Like complex **4**, LSV and CV were the principle analytical techniques used to explore its binding interaction with a variety of anions and biomolecules. As shown in Figure 8A, the LSV profile of complex **6** was significantly altered in the presence of guanine compared to other analytes. The guanine introduced a new peak at -0.252 V and shifted the oxidation potential of complex **6** towards a higher potential. The peak currents for the interfering ions were nearly the same as for guanine oxidation although the oxidation peak of guanine complex was shifted significantly (Figure 8A). A new peak was observed at -0.252 V and the peak current increased linearly with the addition of guanine (inset of Figure 8B). The linear range of detection, limit of detection (LOD) and sensitivity of complex **6** towards guanine were calculated by generating a plot between peak current and concentration of guanine at -0.252 V. A linear relationship was observed in the concentration range from 2.5 to 100 μM and the linear regression equation is $I_{pa}(\mu A) = 0.142C_g(\mu M) + 2.533$, $R^2 = 0.994$ as shown in the inset of Figure 8B. The LOD was calculated using the signal to noise ratio (3σ) method and is about 11.3 nM. To sense the guanine in a real environment, interference studies were performed. Analogous to other complexes, it has good selectivity for guanine in a competing environment (Figure 9 and S12). An analysis of the interference results revealed that complex **6** retains its affinity towards guanine even in the presence of other competing molecules.

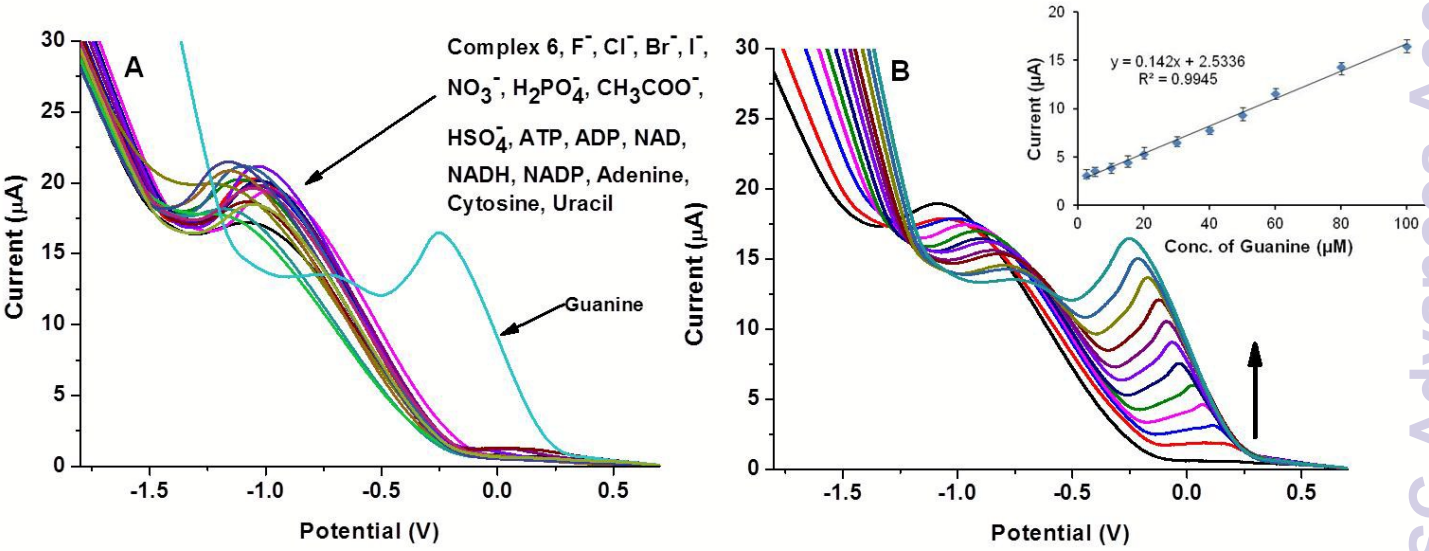

Figure 8. (A) Linear sweep voltammogram of complex **6** (10 μM) in the presence of various tetrabutylammonium anion salts and biomolecules (150 μM) in a THF/H_2O (8:2, v/v) solvent system; (B) Successive changes in the LSV profile of complex **6** upon titration with guanine (0 to 150 μM), the inset shows the plot between the current at -0.252 V and the concentration of guanine.

View Article Online
DOI: 10.1039/C4RA12892C

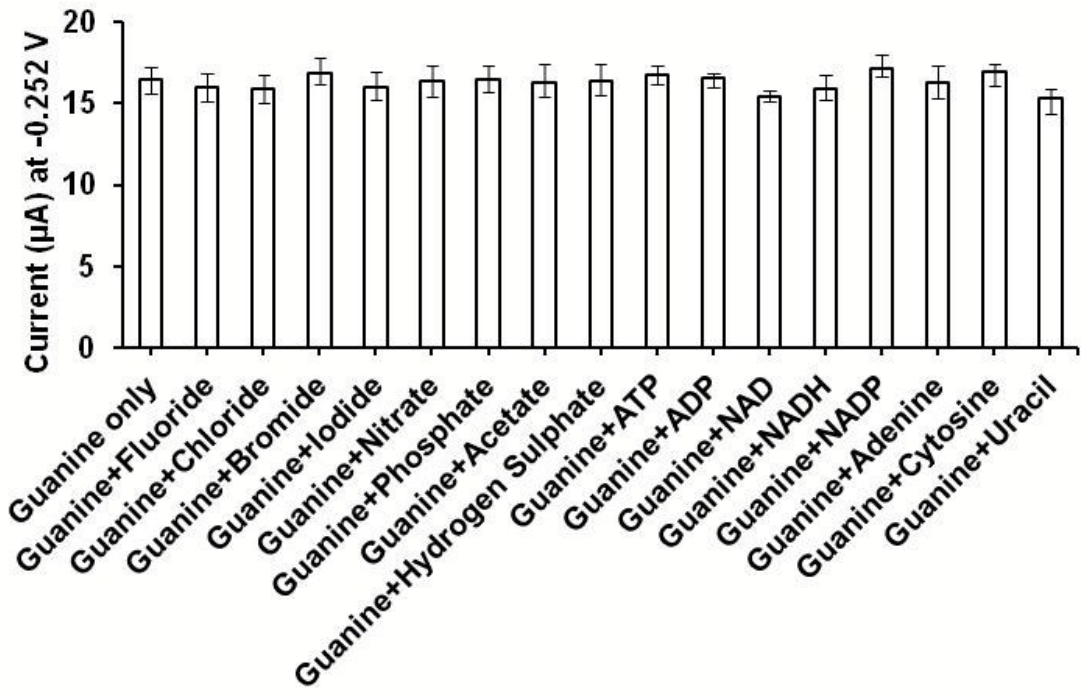

Figure 9. Interference study of complex **6** (10 μM) through monitoring the peak current at -0.252 V in the presence of guanine along with equal molar of various competing anions and biomolecules in THF/H_2O (8:2, v/v).

For further clarification and to support the LSV results, binding studies were performed using the CV technique. The cyclic voltammograms of complex **6**, complex **6** + guanine, and guanine only were recorded in a THF/H_2O (8:2, v/v) solvent system to prove the selectivity (Figure 10A). Complex **6** exhibited a well-defined reversible redox couple with a cathodic potential at -1.023 V and anodic potential at -1.082 V. The addition of guanine produced significant changes in redox potential at -0.813/-0.801 V with an enhancement in the anodic peak current. Both oxidation and reduction peaks moved towards higher potential in the presence of guanine. The voltammogram of a blank solution containing guanine only matched neither with complex **6** nor complex **6** + guanine, supporting the specific binding between complex **6** and guanine. As an in-depth study, titration was used and it was found that the anodic peak current was linearly dependent upon the concentration of guanine (5-80 μM), as shown in the inset of Figure 10B. It is noteworthy to mention here that there is a large shift in the anodic potential (ΔE_{pa} = 275 mV) as well as in the cathodic potential (ΔE_{pa} = 210 mV) during titration. However, the cathodic peak current decreased and the anodic peak current increased with guanine addition. The cyclic voltammograms of complex **6** were recorded at different scan rates (25, 50, 75, 100 and 120). The linear relationship was observed between peak current and square root of scan rate, indicating a diffusion process (Figure 11).

View Article Online
DOI: 10.1039/C4RA12892C

Non-specific adsorption on working electrode may lead to electrode fouling and poor reproducibility. To examine the antifouling property of the working electrode, cyclic voltammograms of complexes **2**, **4** and **6** were recorded at different interval of time. The profiles remained the same even after 25 min with a small decrease in current intensity, eliminating the possibility of non-specific adsorption on working electrode or electron fouling (Figure S13). For optimization, pH titrations of complexes **2**, **4** and **6** were performed. The peak current of complexes **2**, **4** and **6** remained constant and highest in the pH range of 4.5 to 10. Going beyond these limits in either direction led to a decrease in peak current. Therefore, all studies were performed at pH 7.5 ± 0.2.

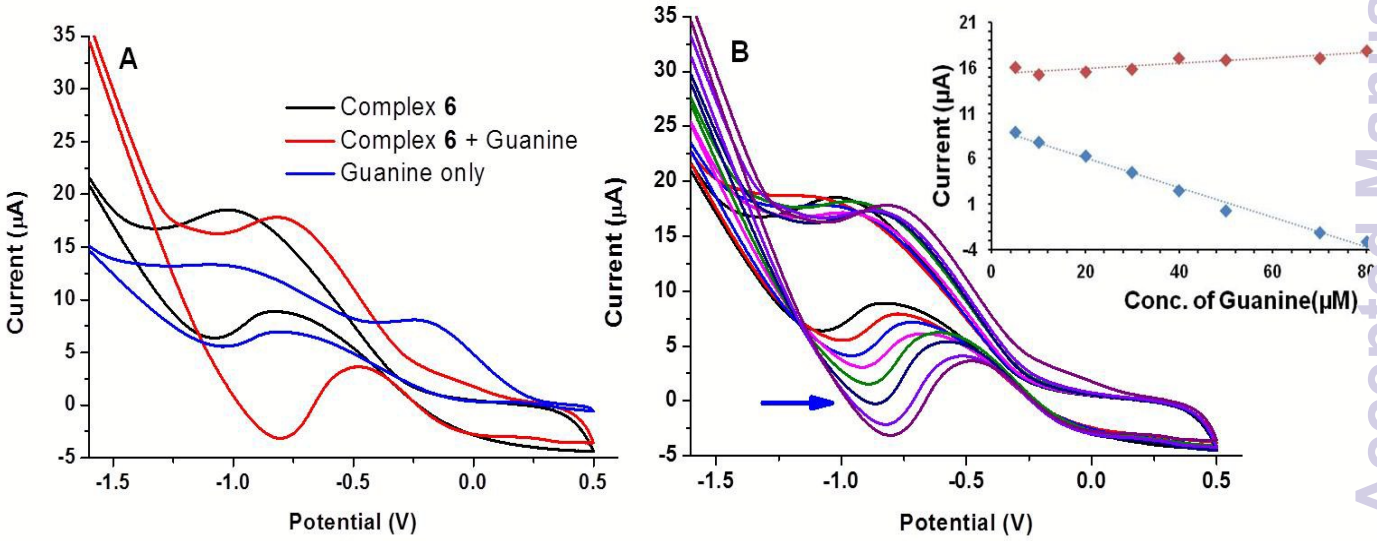

Figure 10. (A) Comparison of the cyclic voltammogram of complex **6** (10 μM), complex **6** + guanine (80 μM), and guanine only (50 μM) (blank) in a THF/H_2O (8:2, v/v) solvent system; (B) Gradual changes in the redox potential of complex **6** (10 μM) upon successive addition of guanine (0 to 80 μM). The inset depicts the linear relationship between the cathodic/anodic peak current at -0.813/-0.801 V and concentration of guanine (5 to 80 μM). Blue points represent the change in anodic current and red points represent the change in cathodic current.

View Article Online
DOI: 10.1039/C4RA12892C

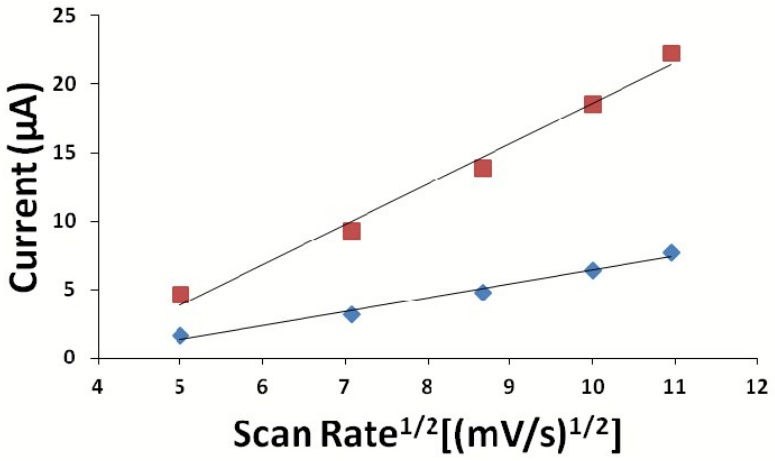

Figure 11. Calibration plot of complex **6** showing peak current versus square root of scan rate (25, 50, 75, 100 and 120). Blue points represent current at -1.078 V and red points represent the current at -1.028 V.

Comparison of analytical performance of complexes 2, 4 and 6

Complexes **2**, **4** and **6** are Co(III) complexes of benzimidazole/benzothiazole, which are enriched with H-bonding sites. Consequently, the driving force behind the sensing of guanine is H-bonding. They are similar in structure and all have similar selectivity towards guanine. It was interesting to compare analytical parameters, such as LOD, the linear range of detection, and sensitivity of complexes **2**, **4** and **6**. A comparison was made and it was found that all three have a limit of detection in the nanomolar range, as shown in Table 1. Among them, complex **4** has a wide linear range of detection and good sensitivity. Furthermore, a comparison was made between the present work and the reported literature, showing that the analytical data of complexes **2**, **4** and **6** are comparable with previous publications. For reproducibility, the relative standard deviation (RSD) of complex **2** (3.2 %), complex **4** (3.3 %) and complex **6** (3.1 %) was calculated (n = 7).

Table 1. Comparison of the analytical parameters of different methods for guanine detection.

Electrode	Technique*	Linear detection range	LOD (nM)	Ref.
Complex **2**	DPV	3.5-10 μM	16.6	Present work
Complex **4**	LSV	5.0-120 μM	13.4	Present work
Complex **6**	LSV	2.5-100 μM	11.3	Present work
Cobalt oxide nanostructure-modified glass carbon electrode	Amperometry	40 nM-10 μM	3	[19]
Cobalt hexacyanoferrate-modified	CV	0-4 μg	340	[16]

carbon paste electrode				
Cobalt(II) phthalocyanine-modified carbon paste electrode	DPV	-	550	17
Ionic liquid-carbon nanotube-gold nanoparticles composite film coated electrode	DPV	8 nM-2 mM	5	25
Carbon screen-printed electrode	DPV	-	200	26
β-Cyclodextrin incorporated carbon nanotube-modified carbon paste electrode modified electrode	DPV	200 nM-20μM	200	27

*LSV= Linear sweep voltammetry, DPV= Differential pulse voltammetry, CV= Cyclic voltammetry.

Conclusions

Benzimidazole/benzothiazole-based imine-linked Co(III) complexes **2**, **4** and **6** were prepared, and their electrochemical properties were studied. Co(III) complexes **2**, **4** and **6** showed high selectivity for the electrochemical recognition of guanine. Complex **2** is a differential pulse voltammetric sensor while complexes **4** and **6** are linear sweep voltammetric sensors for nano-molar detection of guanine. The complexes recognize guanine with high selectivity even in the presence of an equal equivalent of other competing molecules. The complexes have a wide operational pH range. The novelty of this work is the unmodified electrode, which was used for the detection of guanine with high selectivity, sensitivity and a low detection limit.

Supporting Information

PXRD, copies of NMR and mass spectra of receptors and their cobalt complexes.

Acknowledgments

This work was supported by the Korean and Indian Government for the India-Korea Joint Program of Cooperation in Science & Technology (NRF-2011-0027710) and the CSIR project (project no: 01(2417)/10/EMR-II).

References

1. P. D. Beer, P. A. Gale, *Angew. Chem. Int. Ed.,* 2001, **113**, 502.
2. E. J. O'Neil, B. D. Smith, *Coord. Chem. Rev.,* 2006, **250**, 3068.
3. L. Fabbrizzi, M. Licchelli, G. Rabaioli, A. Taglietti, *Coord. Chem. Rev.,* 2000, **205**, 85.
4. H.-L. Zhang, X.-L. Wei, Y. Zang, J.-Y. Cao, S. Liu, X.-P. He, Q. Chen, Y.-T. Long, J. Li, G.-R. Chen, K. Chen, *Adv. Mater.,* 2013, **25**, 4097.
5. K.-B. Li, Y. Zang, H. Wang, J. Li, G.-R. Chen, T. D. James, X.-P. He, H. Tian, *Chem. Commum.,* 2014, **50**, 11735.
6. X.-P. He, R.-H. Li, S. Maisonneuve, Y. Ruan, G.-R. Chen, J. Xie, *Chem. Commum.,* 2014, **50**, 14141.
7. X.-P. He, X.-W. Wang, X.-P. Jin, H. Zhou, X.-X. Shi, G.-R. Chen, Y.-T. Long, *J. Am. Chem. Soc.,* 2011, **133**, 3649.

8. Z. Li, S.-S. Deng, Y. Zang, Z. Gu, X.-P. He, G.-R. Chen, K. Chen, T. D. James, J. Li, Y.-T. Long, *Sci. Rep.,* 2013, **3**, 2293.
9. J. Rebek, B. Askew, P. Ballester, C. Buhr, S. Jones, D. Nemeth, K. Williams, *J. Am. Chem. Soc.,* 1987, **109**, 5033.
10. S. J. Lee, D. R. Bae, W. S. Han, S. S. Lee, J. H. Jung, *Eur. J. Inorg. Chem.,* 2008, **2008**, 1559.
11. M. J. Kim, H. Sharma, N. Singh, D. O. Jang, *Inorg. Chem. Commun.,* 2013, **36**, 96.
12. Y. Zhou, Z. Xu, J. Yoon, *Chem. Soc. Rev.,* 2011, **40**, 2222.
13. E. L. L. Roberts, R. P. Newton, *Anal. Biochem.,* 2004, **324**, 250.
14. N. M. Grubor, R. Shinar, R. Jankowiak, M. D. Porter, G. J. Small, *Biosens. Bioelectron.,* 2004, **19**, 547.
15. S.-H. Lu, S. Selvi, J.-M. Fang, *J. Org. Chem.,* 2006, **72**, 117.
16. A. Abbaspour, M. A. Mehrgardi, *Anal. Chem.,* 2004, **76**, 5690.
17. A. Abbaspour, M. A. Mehrgardi, R. Kia, *J. Electroanal. Chem.,* 2004, **568**, 261.
18. Z. Gao, *Sens. Actuator B-Chem.,* 2007, **123**, 293.
19. R. Hallaj, A. Salimi, *Anal. Methods,* 2011, **3**, 911.
20. U. Fegade, H. Sharma, N. Singh, S. Ingle, S. Attarde, A. Kuwar, *J. Lumines.,* 2014, **149**, 190.
21. H. Sharma, V. K. Bhardwaj, N. Kaur, N. Singh, D. O. Jang, *Tetrahedron Lett.* 2013, **54**, 5967.
22. H. Sharma, H. J. Guadalupe, J. Narayanan, H. Hofeld, T. Pandiyan, N. Singh, *Anal. Methods,* 2013, **5**, 3880.
23. M. J. Johnson, D. G. Peters, *Electrochemistry of Cobalt-containing Species. Encyclopedia of Electrochemistry*, Wiley-VCH Verlag GmbH & Co. KGaA. 2007.
24. D. P. Manica, Y. Mitsumori, A. G. Ewing, *Anal. Chem.,* 2003, **75**, 4572.
25. F. Xiao, F. Zhao, J. Li, L. Liu, B. Zeng, *Electrochim. Acta,* 2008, **53**, 7781.
26. A. Abbaspour, L. Baramakeh, S. M. Nabavizadeh, *Electrochim. Acta,* 2007, **52**, 4798.
27. Z. Wang, S. Xiao, Y. Chen, *J. Electroanal. Chem.,* 2006, **589**, 237.